DOI: 10.1021/ma902601d

Macromolecules
ARTICLE

Re-examination of the "Zipper Effect" in Hydrogen-Bonding Complexes

Lin Deng, Chunhao Wang, Zi-Chen Li,* and Dehai Liang*

Beijing National Laboratory for Molecular Sciences and the Key Laboratory of Polymer Chemistry and Physics of the Ministry of Education, College of Chemistry and Molecular Engineering, Peking University, Beijing 100871, P. R. China

Received November 28, 2009; Revised Manuscript Received February 3, 2010

ABSTRACT: Using poly(acrylic acid) (PAA) and polyacrylamide (PAAm) as an example, we studied the mechanism of hydrogen-bonding complexation in dilute solution by both static and dynamic light scattering. In 20 mM phosphate buffer at pH = 3, the condition suitable for complexation of PAA and PAAm, neither PAA nor PAAm stayed as individual polymer chains at 8.0 mg/mL. Instead, most of PAA formed "multimacroion clusters" (or slow mode) due to the negative charges, and a small portion of PAAm formed associates mainly via hydrogen bonds. After PAA and PAAm solutions were mixed at stoichiometric ratio at room temperature, the slow mode, with PAA being dominant, persisted. The hydrogen-bonding complexation induced by cooling was evolved from the slow mode rather than from the single PAA or PAAm chains. Therefore, at the temperature where phase separation occurred, a fairly large amount of free PAAm chains still existed in the system. Our study demonstrated that the growth of the hydrogen-bonding complex, as well as the optimal ratio for complex, was highly dependent on the status of the component polymers before complexation.

Introduction

Interpolymer complexes, which are formed by secondary binding forces, such as electrostatic interaction, hydrophobic interaction, van der Waals forces, and hydrogen bonds, have been extensively investigated and keep attracting increasing attentions.[1−4] Not only are the interpolymer complexes able to be used as new kinds of polymer materials exhibiting properties and functions totally different from the component polymers, the study on the complexation of synthetic polymers also gains insight into the interactions of biomacromolecules in living cells and consequently the characteristics and functions of biological systems.[5−8] On the basis of the main binding forces, the interpolymer complexes could be divided into four classes: polyelectrolyte complexes, hydrogen-bonding complexes, stereocomplexes, and charge-transfer complexes.[6]

The hydrogen-bonding complexes are limited to the proton-donating and proton-accepting polymer pairs. Generally, the proton-donating polymers were weak polymeric acids, mainly poly(acrylic acid) (PAA) and poly(methacrylic acid) (PMAA), while the proton-accepting polymers were nonionic polymers,[9,10] such as poly(ethy1ene oxide) (PEO),[4,8,11,12] poly(vinylpyrrolidone) (PVP),[13−15] poly(vinyl methyl ether) (PVME),[16] poly(vinyl alcohol) (PVA),[10] poly(*N*-isopropylacrylamide) (PNIPAAM),[16] poly(2-hydroxyethyl vinyl ether) (PHEVE),[17] hydroxypropylcellulose (HPC),[18−20] hydroxyethylcellulose (HEC),[21] and poly(ethylene imine) (PEI).[22] The interaction of the two polymers is almost stoichoimetry.[6] The factors affecting the structure and stability of the complexes, such as concentration, pH, ionic strength, stoichiometric ratio, and structures of the two complementary polymers,[15,23,24] have been investigated and documented. Recently, the hydrogen-bonding complexes find the application as drug carriers[25−29] in the format of interpenetrating polymer networks (IPN).[30,31] Focused on but not limited to PAA/PAAm, several research groups have spent effort to explore the formation mechanism,[32−40] the physical and chemical properties, and the phase separation behavior of the IPNs[30,31] formed by hydrogen-bonding complexes. On the contrary to the well-studied thermoresponsive poly(*N*-isopropylacrylamide) hydrogels,[41] the IPN of PAA/PAAm exhibited the behavior with upper critical solution temperature (UCST),[6,25,42] where the hydrogen-bonding complex shrinks and eventually phase separates (or precipitates) with decreasing temperature.

Detailed study on the complexation of PAA and PAAm helps to understand the phase behavior of the IPN they formed. It has been reported that PAA and PAAm form stable complexes at pH < 4, in which situation the degree of ionization of PAA is low.[32] Under such conditions, the complex formation is via hydrogen bonds as well as the ion-dipole interactions between some of the amide groups of PAAm which is partially protonated and the C═O dipoles of the carboxyl groups of PAA.[2,6,34] Therefore, increasing salt concentration tends to decrease the stability of formed complexes because of the screening of the ion−dipole interactions and the enhanced dissociation of PAA.[2,6,34] Nevertheless, it is commonly believed that PAA and PAAm form complex via "zipper effect" at lower pH and weak ion strength.[32,34,43]

The "zipper effect" is based on the assumption that both PAA and PAAm stay as individual chains before complexation. However, it has been well-established in the literature that polyelectrolytes, even ionomers, formed "multimacroion domains"[44−50] in salt-free or low-salt solution. When polyelectrolyte or ionomer is studied by dynamic light scattering in dilute solution, two diffusive relaxation modes, with none of the mode representing the diffusion of the single polymer chain, are observed. The fast mode is attributed to the coupled diffusion of polyion/counterions,[50−55] while the interpretation of the slow mode has not reached an agreement.[46−48] Since the slow mode disappears at elevated salt concentration, the major driving force is attributed to electrostatic interactions. Herein, we used "multimacroion domains (or clusters)" to denote such associate. At pH = 3, PAA dissociates slightly, which should result in the

*Corresponding authors: e-mail dliang@pku.edu.cn, Tel (+86)10-62756170 (D.L.); e-mail zcli@pku.edu.cn, Tel (+86)10-62753353 (Z.-C.L.).

 Published on Web 02/17/2010

formation of macroion domains. Sedlák has demonstrated that PAA exhibited bimodal distribution in pure water.[56] Besides the formation of "multimacroion domains", PAAm and PAA at neutral state have the ability to form interchain hydrogen bonds, leading to further association of PAAm and PAA. However, the association of the component polymers and its effect on the hydrogen-bonding complexation has not been reported in the literature.

Therefore, in this work, we synthesized both PAA and PAAm with narrow molecular weight distribution by "living"/controlled polymerization and determined their behavior in 20 mM phosphate buffer, whose pH value (=3.0) and ion strength were suitable for complex formation. Our laser light scattering (LLS) results clearly indicated that neither PAA nor PAAm stayed as single polymer chains under such conditions. Upon forming complex, the "slow mode" exhibited direct effect on the size and structure of the complexes. We also found that the "slow mode" remained at different concentrations and in the situation when PAA with varying chain length was employed.

Experimental Section

Materials. *tert*-Butyl acrylate (*t*BA, Aldrich, 98%) was distilled in the presence of calcium hydride. Acrylamide (AAm) was recrystallized from chloroform. 4,4′-Azobis(4-cyanopentanoic acid) (V-501, ACROS, 97%), ethyl 2-bromo-2-methylpropanoate (EBiB, J.T. Baker Backer grade), trifluoroacetic acid (Alfa Aesar, 99%), and copper(I) bromide (CuBr, Aldrich, 99.999%) were used as received. *N*,*N*,*N*′,*N*″,*N*″-Pentamethyldiethylenetriamine (PMDETA, Aldrich, 99%) was dried over calcium hydride and distilled under reduced pressure. Methyl 2-(ethoxycarbonothioylthio)propanoate (chain transfer agent, CTA) was synthesized according to a known procedure.[57] Milli-Q water (Millipore) with resistance of 18.2 MΩ·cm was used throughout the experiments. Sodium dihydrogen phosphate dihydrate ($NaH_2PO_4 \cdot 2H_2O$) with A.R. grade was purchased from Beijing Chemical Reagents Co. (Beijing, China) and used as received. The phosphate buffer was prepared by dissolving known amount of $NaH_2PO_4 \cdot 2H_2O$ in Milli-Q water. The pH of the buffer was adjusted by 1.0 N HCl.[58]

Synthesis of PAA and PAAm. Poly(*tert*-butyl acrylate) (P*t*BA) was synthesized by atom transfer radical polymerization (ATRP) of *t*BA in anisole with EBiB as the initiator. A typical procedure for the synthesis of P*t*BA-1 was as follows. CuBr (84.4 mg, 0.586 mmol) was added to the mixture of *t*BA (6.0 g, 47 mmol), PMDETA (126.6 μL, 0.586 mmol), EBiB (86.0 μL, 0.586 mmol), and anisole (3.0 g). After degassed by three freeze−pump−thaw cycles, the mixture was sealed under nitrogen and heated at 100 °C for 2.5 h. The solution was diluted with THF and filtered over neutral alumina to remove the copper. The resulting colorless polymer solution was concentrated and precipitated into 70% methanol/water. The white polymer precipitate was collected by vacuum filtration and dried under vacuum for 24 h at room temperature. Three samples of P*t*BA with different molecular weights were prepared following the same procedure but varying the molar ratio of *t*BA to EBiB and the reaction time (Supporting Information, Table S1). The size exclusion chromatography (SEC) traces of the P*t*BA samples are shown as Supporting Information (Figure S1).

PAA was obtained by acid-catalyzed hydrolysis of P*t*BA. A mixture of P*t*BA (5.4 g), dichloromethane (48 mL), and trifluoroacetic acid (42.75 g) was stirred at 30 °C for 24 h. The solvent was then evaporated, and the sample was dissolved in THF, followed by precipitation in petroleum ether. The product was dried under vacuum for 24 h. The complete transformation of the *tert*-butyl ester to the acids was confirmed by ^{1}H NMR via the disappearance of the signal at δ 1.44 ppm (Supporting Information, Figures S2 and S3). The exact molecular weight of PAA was difficult to determine. According to the monomer conversion in Table S1, the degrees of polymerization of three P*t*BA samples were estimated to be 64, 86, and 137. The PAAs are correspondingly denoted as PAA64, PAA86, and PAA137, respectively.

PAAm was synthesized by the RAFT polymerization of AAm in isopropanol and water with V-501 as the initiator and methyl 2-(ethoxycarbonothioylthio)propanoate as the CTA. Specifically, a mixture of AAm (10.0 g, 141 mmol), V-501 (22.5 mg, 80 μmol), CTA (84 mg, 0.404 mmol), isopropanol (3.0 g), and water (15.0 g) was degassed by three freeze−pump−thaw cycles, sealed at nitrogen, and heated at 50 °C for 20 h. PAAm was purified and isolated by precipitation from the mother solution in acetone, followed by desiccation under vacuum overnight. The product was lyophilized from water and obtained as white powders with the yield of 75%. The aqueous SEC result is shown in Figure S4. The determined molecular weight $\langle M_n \rangle$ and $\langle M_w \rangle / \langle M_n \rangle$ are 18 700 g/mol and 1.26, respectively. This PAAm sample is thus denoted as PAAm260.

Measurements. The NMR spectra were recorded in $CDCl_3$ on a Bruker ARX-400 spectrometer or a Varian Gemini 300 spectrometer. SEC was carried out in tetrahydrofuran (THF) (flow rate: 1 mL/min) at 35 °C on a Waters 1525 binary HPLC pump equipped with a Waters 2414 refractive index detector and three Waters Styragel HR columns (HT-2, HT-3, HT-4). Monodispersed polystyrene standards were used for calibration. Data were analyzed by Breeze software (version 3.30 SPA). Aqueous size exclusion chromatography was carried out in aqueous solution at 150 mM NaCl (flow rate: 0.8 mL/min) at 35 °C on the same instrument but equipped with three Waters Ultrahydrogel columns (120, 250, 500). Calibration was conducted with linear PEO as the standards.

Zeta Potential Analysis. Zeta potential was measured on the commercial instrument (ZetaPALS) from Brookhaven Instruments Corp. (Holtsville, NY). The measuring conditions, such as concentration and temperature, were the same as those used in LLS.

Laser Light Scattering (LLS). A commercial spectrometer from Brookhaven Instruments Corp. (Holtsville, NY) was used to perform both SLS and DLS over a scattering angular range of 20°−120°. A solid-state laser polarized at the vertical direction (CNI Changchun GXC-III, 532 nm, 100 mW) operating at 532 nm was used as the laser source. In static light scattering, we measured the time-averaged excess scattered intensity at angle θ, also known as the Rayleigh ratio $R_{vv}(q)$. At fixed concentration, it was related with the weight-averaged molar mass $M_{w,app}$, the *Z*-averaged root-mean-square radius $R_{g,app}$, and the scattering vector q as follows:

$$\frac{KC}{R_{vv}(q)} \approx \frac{1}{M_{w,app}}\left(1+\frac{1}{3}R_{g,app}{}^2q^2\right) \quad (1)$$

$$K = 4\pi^2 n^2 (dn/dC)^2/(N_A\lambda_0{}^4) \quad (2)$$

$$q = \frac{4\pi n}{\lambda}\sin\left(\frac{\theta}{2}\right) \quad (3)$$

where N_A, n, (dn/dC), and λ_0 are the Avogadro constant, the refractive index of the solvent, the specific refractive index increment of the solution, and the wavelength of light in vacuum, respectively. The dn/dC values of PAA[59] and PAAm[60] in aqueous solution were 0.16 and 0.18, respectively. Since the two values are very close, we were able to evaluate the $M_{w,app}$ of the complexes by eq 1 with enough accuracy.[61]

In DLS, the intensity−intensity time correlation function $G^{(2)}(\tau)$ in the self-beating mode was measured:

$$G^{(2)}(\tau) = A[1+\beta|g^{(1)}(\tau)|] \quad (4)$$

where A is the measured baseline, β is a coherence factor, τ is the delay time, and $g^{(1)}(\tau)$ is the normalized first-order electric field time correlation function. $g^{(1)}(\tau)$ is related to the line width distribution $G(\Gamma)$ by

$$g^{(1)}(\tau) = \int_0^\infty G(\Gamma)\mathrm{e}^{-\Gamma\tau}\,\mathrm{d}\Gamma \tag{5}$$

The normalized distribution function of the characteristic line width $G(\Gamma)$ was obtained by using a Laplace inversion program, CONTIN. The average line width, $\overline{\Gamma}$, is a function of both C and q, which can be expressed as

$$\overline{\Gamma}/q^2 = D(1+k_\mathrm{d}C)[1+f(R_\mathrm{g}q)^2] \tag{6}$$

where D is the translational diffusive coefficient, k_d is the diffusion second virial coefficient, and f is a dimensionless constant. D can be further converted into the hydrodynamic radius R_h by using the Stokes−Einstein equation

$$R_\mathrm{h} = k_\mathrm{B}T/6\pi\eta D \tag{7}$$

where k_B is the Boltzmann constant, T is the absolute temperature, and η is the viscosity of the solvent.

Sample Preparation. All PAA samples and PAAm were prepared at the same concentration of 8.0 mg/mL in 20 mM phosphate buffer. For LLS and zeta potential measurements, the solution was filtered through a 0.22 μm Millipore filter into a dust-free vial to remove the dust. Upon complexation, known amounts of PAA and PAAm were mixed together to ensure the molarity of AA and AAm groups were equal. Gravimetry was used to make the difference less than 1%. At the chosen pH and concentration, all the mixtures of PAA and PAAm were clear solutions above 30 °C.

Results and Discussion

Association of Polymer Chain. The PAA and PAAm samples in our study were denoted as PAA64, PAA86, PAA137, and PAAm260, with the number denoting the degree of polymerization. For the study on the single chain conformation, we showed the results mainly from PAA86. The other two PAA samples exhibited similar results unless stated otherwise. The molecular weights of PAA and PAAm were low, and the overlap concentrations were in the order of 30−50 mg/mL. We chose 8.0 mg/mL as the starting concentration to facilitate the hydrogen-bond formation. Since the molecular masses of monomer AA (72 g/mol) and AAm (71 g/mol) are close, we prepared PAA and PAAm solution at the same concentration for convenience.

PAA is a weak polyelectrolyte with pK_a about 4.5.[62] At pH = 3.0, it dissociated slightly (~3% ionization) and carried a few negative charges. Considering that the dissociation was a dynamic process, all the acrylic acid group could be charged from time to time. The zeta potential of PAA was determined to be −7.3 ± 1.0 mV at 8.0 mg/mL at 25 °C, suggesting that PAA was negatively charged. Parts A and A′ of Figure 1 show the R_h distribution of PAA86 in phosphate buffer without and with 1.0 N NaCl, respectively. Without NaCl, a bimodal distribution was observed, although the fast mode, with $R_\mathrm{h,app}$ about 3 nm, was much weaker than the slow mode whose $R_\mathrm{h,app}$ was about 67 nm. The fast mode was attributed to the coupled relaxation of the single polymer chains,[63] while the slow mode was attributed to the diffusion of "multimacroion domains". After adding 1.0 N NaCl, the slow mode, on one hand, was significantly suppressed (Figure 1A′), where it was hardly visible at 90°, indicating that the nature of the slow mode resulted mainly from electrostatic interactions. One the other hand, the slow mode at 30° did not disappear, suggesting that 1.0 N NaCl might not strong enough to totally suppress the slow mode. Other possible driving forces for the formation of slow mode at 1.0 N NaCl were the association of PAA caused by the salting out effect as well as the interchain hydrogen-bonding between the uncharged PAA. Because of the suppression of the slow mode, the excess scattered intensity after extrapolation to zero angle was decreased by a factor of about 2 after adding 1.0 N NaCl (data not shown), consistent with the DLS result.

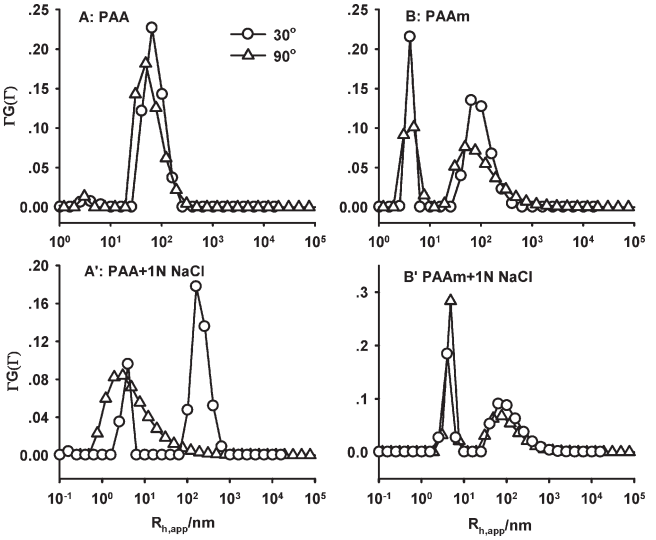

Figure 1. R_h distribution (CONTIN results) of PAA86 (A, A′) and PAAm260 (B, B′) without and with 1.0 N NaCl in phosphate buffer at 8.0 mg/mL at 25 °C.

As shown in Figure 1B, a bimodal distribution was also observed in PAAm260 at 8.0 mg/mL. The fast mode has $R_\mathrm{h,app}$ about 4 nm, which was reasonably attributed to the relaxation of the single polymer chains. The slow mode, with $R_\mathrm{h,app}$ about 85 nm, was probably caused by the interchain hydrogen bonding via the amide groups at the studied concentration. Moreover, our zeta potential measurement indicated that PAAm was positively charged in phosphate buffer at pH = 3.0. Even though the error was large, 11 ± 6 mV should be able to demonstrate the positive charge on PAAm. The positive charge was probably caused by the partial protonation of the amide group at low pH. Therefore, both "multimacroion domains" and association via hydrogen bond could lead to the formation of the slow mode. After adding 1.0 N NaCl, the slow mode was slightly suppressed (Figure 1B). SLS shows that the excess scattered intensity was deceased by 25%, but still much higher than that of single polymer chains, suggesting that the "slow mode" was formed via both mechanisms, and hydrogen bond was the major driving force.[64]

Mixture of PAA86 and PAAm260. As demonstrated above, neither PAA nor PAAm stayed as individual polymer chains in phosphate buffer. When PAA and PAAm were mixed at stoichiometric ratio, i.e., 1:1 AA/AAm molar ratio, hydrogen-bonding complexation should occur at the maximum strength according to the "zipper" mechanism. As shown in Figure 2, a characteristic bimodal distribution was observed in the mixture containing equal amounts of PAA and PAAm, with the total concentration being 8.0 mg/mL. It was interesting that the $R_\mathrm{h,app}$ of the fast mode was 4 nm, close to the value of the fast mode in PAAm sample (Figure 1B), while the $R_\mathrm{h,app}$ of the slow mode was 69 nm, close to the value of the slow mode in PAA solution (Figure 1A).

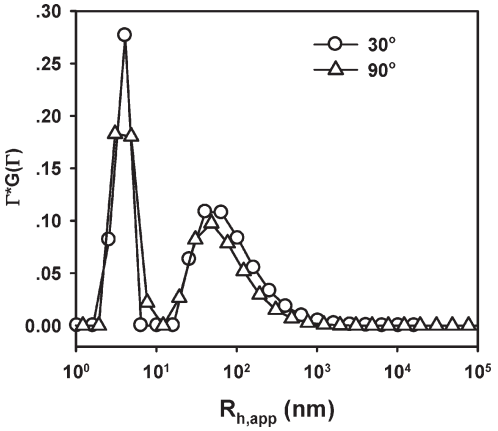

Figure 2. R_h distribution (CONTIN results) of the complex formed by PAA86 and PAAm260 in phosphate buffer at 25 °C. The total concentration was 8.0 mg/mL.

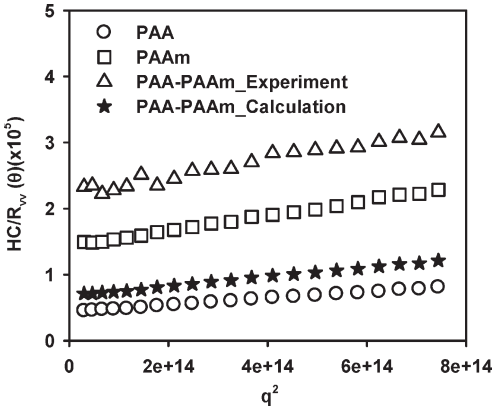

Figure 3. SLS results of PAA86, PAAm260, and PAA86 + PAAm260 in phosphate buffer at 8.0 mg/mL at 25 °C.

Figure 3 compares the angular dependence of the excess scattered intensity (in the form of HC/R_{vv}) of the complex and its components at the same concentration. The $M_{w,app}$ values, which were obtained from the interceptions in the Y-axis, were 2.3×10^5 g/mol for PAA, 8.7×10^4 g/mol for PAAm, and 4.5×10^4 g/mol for the complex. As for PAA or PAAm, the measured $M_{w,app}$ was much larger than that of the single polymer chains, with the former increased roughly by a factor of 370 and the latter by a factor of 5. Since the excess scatted intensity in SLS was proportional approximately to the sixth power of the particle size,[65] the appearance of the slow mode (Figure 1) inevitably led to a sharp increase in the excess scattered intensity and consequently the $M_{w,app}$. Assuming that the mixing did not cause any change on PAA and PAAm, and the excluded volume interaction were the same for PAA and PAAm under the used conditions, the $M_{w,app}$ of the mixture was calculated to be 1.5×10^5 g/mol according to eq 1 in the Experimental Section, which was indicated by the "black stars" in Figure 3. This number was 3 times larger than the measured value (4.5×10^4 g/mol). The decrease in the excess scattered intensity after mixing, as well as the decrease in the $M_{w,app}$, was mainly due to the reduction of the slow mode from both PAA and PAAm (Figure 1). Even though the excess scattered intensity of the complexes was reduced, it was still a few times larger than that of the single PAA or PAAm chains.

It was difficult to determine the nature of the fast mode and slow mode shown in Figure 2 at current stage. The zeta potential of the mixture was determined to be -5.3 ± 0.4 mV,

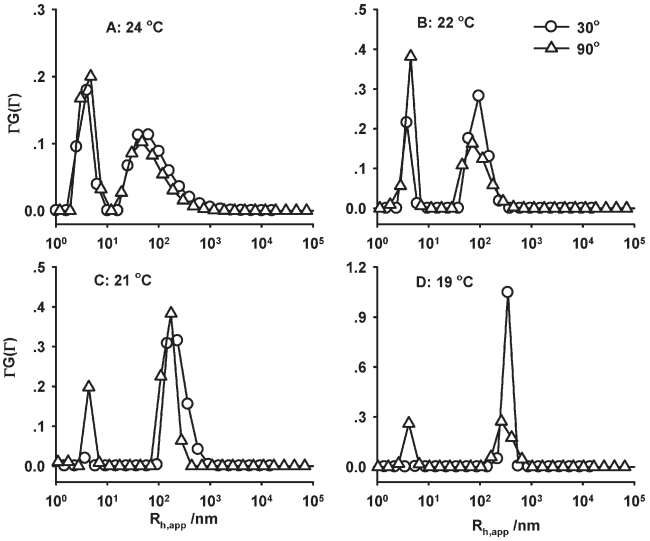

Figure 4. R_h distribution of 8.0 mg/mL PAA86 + PAAm260 in phosphate buffer at different temperatures.

indicating that not all groups from PAA chains formed complex with PAAm. Otherwise, the charge on PAA should be neutralized. Therefore, the slow mode in Figure 2 could be attributed to the mixture of the macroion cluster of PAA, the associate of PAAm, and the partial complex of PAA with PAAm. Since PAA and PAAm carried different charges, their complex was also bonded by the electrostatic interactions (or ion−dipole interaction), in agreement with the findings by Tsuchida et al.[2]

Complexation of PAA86 and PAAm260. Besides pH and concentration, temperature was an effective factor to adjust the complexation. With decreasing temperature, the hydrogen bond between PAA and PAAm was strengthened, leading to a heavy formation of complex. As shown in Figure 4, the bimodal distribution was maintained throughout the cooling process to 19 °C, below which the solution became milky and no valid LLS data were obtained. The major change during cooling was that the size and area ratio of the slow mode sharply increased below 23 °C. Because PAA or PAAm solution at the same concentration exhibited negligible changes during the whole cooling process (Figure S7), the increase in the slow mode of the mixture at lower temperature was caused by the complexation of PAA and PAAm. It was reasonable since lower temperature enhanced the hydrogen bonding between PAA and PAAm.[20,40] Figure 4 also indicated that the hydrogen-bonding complex evolved from the slow mode, instead of the single polymer chains. Otherwise, a gradual growth of the fast mode and a corresponding shrinkage of the slow mode should be observed in the early stage. To further demonstrate this point, we calculated the amplitude ratio of the slow mode to fast mode, A_s/A_f,[66] at varying temperature. As shown in Figure S8, the A_s/A_f sharply increased below 23 °C, above which it kept almost constant. Figure 5A shows the temperature dependence of $R_{h,app}$ after the extrapolation to zero angle. The size of the complex (or the slow mode) continuously increased from about 70 nm at 23 °C to more than 300 nm at 19 °C. At temperatures above 23 °C, no apparent change in size was observed. Figure 5A also shows that the size of the fast mode was kept constant at 4 nm throughout the cooling process. Figure 5B shows the data from SLS. It was clear that the angular dependence of the HC/R_{vv} was determined mainly by the growth of the complex, where a sharp increase in $M_{w,app}$ occurred after 23 °C, agreed well with the data from DLS.

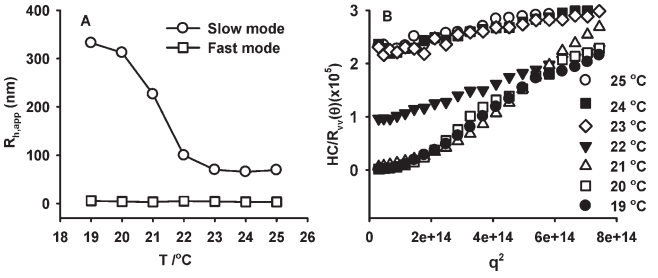

Figure 5. $R_{h,app}$ (A) and angular dependence of HC/R_{vv} (B) of 8.0 mg/mL PAA86 + PAAm260 in phosphate buffer at different temperature.

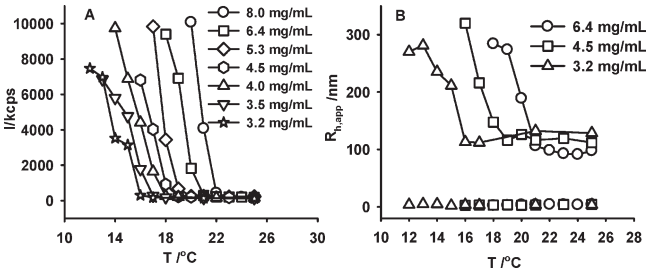

Figure 6. Temperature dependence of the scattered intensity of PAA86 + PAAm260 in phosphate buffer (A) and $R_{h,app}$ (B) of the fast mode and slow mode at selected concentrations.

Figure 5 also shows that the critical complexation temperature (CCT) of PAA and PAAm at stoichiometric ratio was about 22 °C. It was also concentration-dependent. As shown in Figure 6A, the CCT, which was determined from the onset point of the scattered intensity, decreased as the concentration was lowered. It was understandable considering that the dilution had to be compensated by the enhanced interchain hydrogen bonding at lower temperature. At the studied concentration range, the complexation of PAA and PAAm showed similar results. As shown in Figure 6B, the slow mode was kept almost constant before the transition point, while a sharp increase in size and area ratio was observed after the transition point. On the other hand, the fast mode was determined to be 4 nm and independent of the concentration.

The driving force for the complexation of PAA and PAAm could be identified from the thermodynamic analysis of the data in Figure 6. Similar to the treatment on micellization process,[67,68] the free energy $\Delta G°$, enthalpy $\Delta H°$, and entropy $\Delta S°$ of the complexation were related to the critical complex concentration (CCC) as follows:

$$\Delta G° = \Delta H° - T\Delta S° = RT \ln(\mathrm{CCC}) \quad (8)$$

$$\Delta H° = R[\mathrm{d} \ln(\mathrm{CCC})/\mathrm{d}(1/T)] \quad (9)$$

where T is temperature and CCC is in molar concentration. Assuming that enthalpy is independent of temperature, eq 8 takes a simple form

$$\ln(\mathrm{CCC}) = (\Delta H°/RT) + k \quad (10)$$

with k being a constant. The CCC values at given temperature were retrieved from Figure 6. The plot of CCC vs T^{-1} is shown in Figure 7. $\Delta H°$ was thus determined to be -120 kJ/mol at the studied temperatures range. At 22 °C, eq 1 yielded $\Delta G°$ of -19 kJ/mol and $\Delta S°$ of -340 J/(mol K). $\Delta H° < 0$ and $\Delta S° < 0$ indicated that the complexation of PAA and PAAm was an enthalpy-driven process with a loss in configurational entropy, which agreed with the results determined

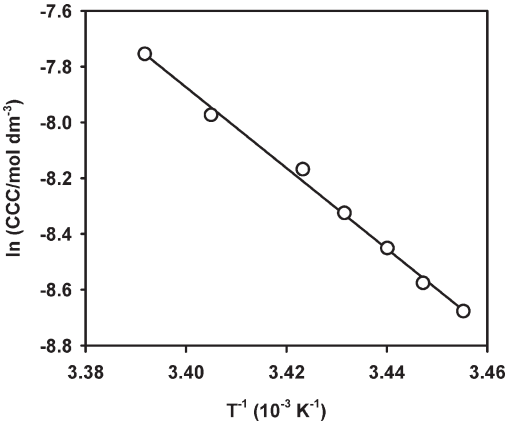

Figure 7. Plot of the logarithmic critical aggregation concentration versus the reciprocal of the absolute temperature for the PAA86 + PAAm260 complex in phosphate buffer.

via potentiometric measurement by Staikos et al.[40] The complexation of PAA and PAAm followed similar rules as the micellization of block copolymers in organic solvents, such as poly(styrene)-*b*-poly(*tert*-butylstyrene) in *N*,*N*-dimethylacetamide[67] and polystyrene-*b*-polyisoprene in *n*-hexadecane,[68] where both negative $\Delta H°$ and $\Delta S°$ were observed. As for the hydrogen-bonding complexes formed by PAA (or its derivatives, poly(methacrylic acid)) and poly(ethylene oxide) in aqueous solution, positive values of $\Delta H°$ and $\Delta S°$ were usually obtained,[4,69] indicating that hydrophobic interactions was the major driving force. This is probably the reason that the hydrogels with UCST behavior was based mainly on PAA/PAAm instead of PAA/PEO, even though PEO possessed better biocompatibility.

Even though the thermodynamic analysis was rough, it indicated that the complexation of PAA and PAAm was enthalpy-driven, which was demonstrated as the growth of the slow mode shown in Figure 4. The attractive interaction between PAA and PAAm, on the basis of the $\Delta H°$ and $\Delta S°$ values, was mainly interchain hydrogen-bonding. Ion−dipole interaction or electrostatic interaction also played a role, but not dominant, since such interactions usually led to an increase in entropy because of the release of counterions.[6]

Effect of PAA Length on Complexation. To determine the nature of the fast mode with $R_{h,app}$ of 4 nm, we studied the thermo-induced complexation of PAAm and PAA with different chain length. As expected,[5,6,33,70] PAA with longer chain showed stronger complexation ability with PAAm at the same conditions, i.e., 8.0 mg/mL total concentration and 1:1 AA/AAm ratio. As demonstrated in Figure 8A, the transition point increased with increasing chain length of PAA. During complexation, the characteristic bimodal distribution was observed in all the three PAA samples (Figure S6). Figure 8B compares the fast mode and slow mode during the cooling process. It was clear that the fast mode was independent of the PAA chain length. Further considering that the fast mode was also independent of concentration and temperature, and its size and size distribution were close to those of single PAAm, we attribute the fast mode to the free PAAm chains in the system. Since the excess scattered intensity was proportional roughly to the sixth power of particle size, the intensity-averaged $R_{h,app}$ distribution (e.g., Figure 4) implied that fairly large amount of PAAm chains did not participate in the complex formation, even at temperatures far below the transition point (e.g., Figure 4D). This definitely not caused by the error of feed ratio since we have balanced the molar ratio of AA/AAm to double digits

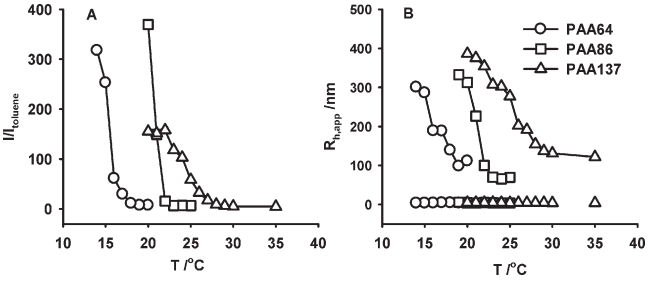

Figure 8. Temperature dependence of the scattered intensity (A) and $R_{h,app}$ (B) of PAAm260 complexing with PAA of different chain length.

precision (< 1%). The existence of free PAAm chains suggested that the complex formed by PAA and PAAm was not at 1:1 monomer ratio. In other words, the "zipper" mechanism of hydrogen-bonding complexation may not apply to the whole complexation process.

On the basis of the above results, we further explain the complexation of PAA/PAAm as follows. In phosphate buffer, not all the PAA or PAAm stayed as individual polymer chains. PAA chains formed multimacroion domain and PAAm chains also form associates (Figure 1). Upon mixing together, the macroion cluster and the PAAm associates were weakened probably due to certain screening or dilution effect, but they did not disappear (Figures 2 and 3). Moreover, they served as the precomplex, where the amount of PAA was much more than that of PAAm; i.e., they were not in the regulated molar ratio for "zipper" structure. At the temperature where the interchain complex via hydrogen-bonding or ion−dipole interaction started to occur, the size and the density of the precomplex started to grow, with more PAAm chains involved in the complex (Figure 4). The "zipper" structures with limited length could be formed during this stage, but the amount could be low since free PAAm chains still existed in the system after phase separation. Therefore, PAA played the leading role during the complex formation mainly because of the multimacroion domain, not the chain length.

Conclusion

The mechanism of hydrogen-bonding complexation was more complicated than expected. The complication was derived from the association of component polymers before mixing. Using PAA and PAAm as the example, we demonstrated that both of the two-component polymers formed associates or "multimacroion domains" (also referred to as slow mode) at the conditions suitable for complexation. After mixing, the hydrogen-bonding complex was evolved from the slow mode instead of the single polymer chains. Therefore, the slow mode played a key role in determining the structure and physical properties of the formed complexes. As for the complex formed by PAA and PAAm at stoichiometric ratio, a fairly large amount of free PAAm chains was not involved in complexation since the slow mode was dominated by PAA.

Our results should also apply to the polyelectrolyte complexation at low salt concentrations. The first realization of the slow mode of polyelectrolyte was in 1978,[50] decades later than the study on interpolyelectrolyte complexation,[6] and the interpretation of the slow mode was still controversial. It was probably the reason that the effect of slow mode on the complexation was ignored. Moreover, the interpolymer complexes generally involved multiple interactions and were controlled by both thermodynamics and kinetics. A proper control on the association of the component polymers before mixing was crucial to develop interpolymer complex with novel properties and desirable features.

Acknowledgment. Financial support of this work from the National Natural Science Foundation of China (20774004) was gratefully acknowledged.

Supporting Information Available: ^{1}H NMR spectra and GPC results on PAA and PAAm; size distribution of PAA86, PAAm260, PAA137 + PAAm260, and PAA64 + PAAm260 at different temperatures. This material is available free of charge via the Internet at http://pubs.acs.org.

References and Notes

(1) Ilmain, F.; Tanaka, T.; Kokufuta, E. *Nature* **1991**, *349*, 400–401.
(2) Abe, K.; Koide, M.; Tsuchida, E. *Macromolecules* **1977**, *10*, 1259–1264.
(3) Higashi, N.; Nojima, T.; Niwa, M. *Macromolecules* **1991**, *24*, 6549–6551.
(4) Bednar, B.; Li, Z. M.; Huang, Y. H.; Chang, L. C. P.; Morawetz, H. *Macromolecules* **1985**, *18*, 1829–1833.
(5) Bekturov, E.; Bimendina, L. *Adv. Polym. Sci.* **1981**, *41*, 99–147.
(6) Tsuchida, E.; Abe, K. *Adv. Polym. Sci.* **1982**, *45*, 1–119.
(7) Ghiggino, K. P.; Roberts, A. J.; Phillips, D. *Adv. Polym. Sci.* **1981**, *40*, 69–167.
(8) Heyward, J. J.; Ghiggino, K. P. *Macromolecules* **1989**, *22*, 1159–1165.
(9) Nurkeeva, Z. S.; Mun, G. A.; Khutoryanskiy, V. V. *Macromol. Biosci.* **2003**, *3*, 283–295.
(10) Nurkeeva, Z. S.; Mun, G. A.; Dubolazov, A. V.; Khutoryanskiy, V. V. *Macromol. Biosci.* **2005**, *5*, 424–432.
(11) Bednar, B.; Morawetz, H.; Shafer, J. A. *Macromolecules* **1984**, *17*, 1634–1636.
(12) Vasilescu, M.; Anghel, D. F.; Almgren, M.; Hansson, P.; Saito, S. *Langmuir* **1997**, *13*, 6951–6955.
(13) Chen, H. L.; Morawetz, H. *Eur. Polym. J.* **1983**, *19*, 923–928.
(14) Nurkeeva, Z. S.; Mun, G. A.; Khutoryanskiy, V. V.; Bitekenova, A. B.; Dubolazov, A. V.; Esirkegenova, S. Z. *Eur. Phys. J. E* **2003**, *10*, 65–68.
(15) Iliopoulos, I.; Audebert, R. *Macromolecules* **1991**, *24*, 2566–2575.
(16) Khutoryanskiy, V. V.; Mun, G. A.; Nurkeeva, Z. S.; Dubolazov, A. V. *Polym. Int.* **2004**, *53*, 1382–1387.
(17) Mun, G. A.; Khutoryanskiy, V. V.; Akhmetkalieva, G. T.; Shmakov, S. N.; Dubolazov, A. V.; Nurkeeva, Z. S.; Park, K. *Colloid Polym. Sci.* **2004**, *283*, 174–181.
(18) Bumbu, G. G.; Vasile, C.; Eckelt, J.; Wolf, B. A. *Macromol. Chem. Phys.* **2004**, *205*, 1869–1876.
(19) Dubolazov, A. V.; Nurkeeva, Z. S.; Mun, G. A.; Khutoryanskiy, V. V. *Biomacromolecules* **2006**, *7*, 1637–1643.
(20) Lu, X. H.; Hu, Z. B.; Schwartz, J. *Macromolecules* **2002**, *35*, 9164–9168.
(21) Bo, Y. J.; Khutoryanskiy, V. V.; Mun, G. A.; Nurkeeva, Z. S. *J. Polym. Sci., Ser. A* **2002**, *44*, 1094–1098.
(22) Vasheghani, B.; Rajabi, F. H.; Ahmadi, M. H.; Nouhi, S. *Polym. Bull.* **2006**, *56*, 395–404.
(23) Kaczmarek, H.; Szalla, A.; Kaminska, A. *Polymer* **2001**, *42*, 6057–6069.
(24) Prevysh, V. A.; Wang, B. C.; Spontak, R. J. *Colloid Polym. Sci.* **1996**, *274*, 532–539.
(25) Katono, H.; Maruyama, A.; Sanui, K.; Ogata, N.; Okano, T.; Sakurai, Y. *J. Controlled Release* **1991**, *16*, 215–227.
(26) Gil, E. S.; Hudson, S. A. *Prog. Polym. Sci.* **2004**, *29*, 1173–1222.
(27) Alarcon, C. D. H.; Pennadam, S.; Alexander, C. *Chem. Soc. Rev.* **2005**, *34*, 276–285.
(28) Jeong, B.; Gutowska, A. *Trends Biotechnol.* **2002**, *20*, 305–311.
(29) Qiu, Y.; Park, K. *Adv. Drug Delivery Rev.* **2001**, *53*, 321–339.
(30) Dai, H. J.; Chen, Q.; Qin, H. L.; Guan, Y.; Shen, D. Y.; Hua, Y. Q.; Tang, Y. L.; Xu, J. *Macromolecules* **2006**, *39*, 6584–6589.
(31) Owens, D. E.; Jian, Y. C.; Fang, J. E.; Slaughter, B. V.; Chen, Y. H.; Peppas, N. A. *Macromolecules* **2007**, *40*, 7306–7310.
(32) Garces, F. O.; Sivadasan, K.; Somasundaran, P.; Turro, N. J. *Macromolecules* **1994**, *27*, 272–278.
(33) Endo, N.; Shirota, H.; Horie, K. *Macromol. Rapid Commun.* **2001**, *22*, 593–597.
(34) Sivadasan, K.; Somasundaran, P.; Turro, N. J. *Colloid Polym. Sci.* **1991**, *269*, 131–137.
(35) Moharram, M. A.; Balloomal, L. S.; ElGendy, H. M. *J. Appl. Polym. Sci.* **1996**, *59*, 987–990.

(36) Moharram, M. A.; Rabie, S. M.; El-Gendy, H. M. *J. Appl. Polym. Sci.* **2002**, *85*, 1619–1623.
(37) Moharram, M. A.; El-Gendy, H. M. *J. Appl. Polym. Sci.* **2002**, *85*, 2699–2705.
(38) Mun, G. A.; Nurkeeva, Z. S.; Khutoryanskiy, V. V.; Sarybayeva, G. S.; Dubolazov, A. V. *Eur. Polym. J.* **2003**, *39*, 1687–1691.
(39) Staikos, G.; Bokias, G.; Karayanni, K. *Polym. Int.* **1996**, *41*, 345–350.
(40) Staikos, G.; Karayanni, K.; Mylonas, Y. *Macromol. Chem. Phys.* **1997**, *198*, 2905–2915.
(41) Schild, H. G. *Prog. Polym. Sci.* **1992**, *17*, 163–249.
(42) Eustace, D. J.; Siano, D. B.; Drake, E. N. *J. Appl. Polym. Sci.* **1988**, *35*, 707–716.
(43) Sivadasan, K.; Somasundaran, P. *J. Polym. Sci., Polym. Chem.* **1991**, *29*, 911–914.
(44) Sedlak, M.; Amis, E. J. *J. Chem. Phys.* **1992**, *96*, 826–834.
(45) Sedlak, M.; Amis, E. J. *J. Chem. Phys.* **1992**, *96*, 817–825.
(46) Förster, S.; Schmidt, M. *Adv. Polym. Sci.* **1995**, *120*, 51–133.
(47) Prabhu, V. M. *Curr. Opin. Colloid Interface Sci.* **2005**, *10*, 2–8.
(48) Yethiraj, A. *J. Phys. Chem. B* **2009**, *113*, 1539–1551.
(49) Zhou, K. J.; Li, J. F.; Lu, Y. J.; Zhang, G. Z.; Xie, Z. W.; Wu, C. *Macromolecules* **2009**, *42*, 7146–7154.
(50) Lin, S. C.; Lee, W. I.; Schurr, J. M. *Biopolymers* **1978**, *17*, 1041–1064.
(51) Muthukumar, M. *J. Chem. Phys.* **1996**, *105*, 5183–5199.
(52) Sedlak, M.; Konak, C.; Stepanek, P.; Jakes, J. *Polymer* **1987**, *28*, 873–880.
(53) Schmitz, K. S.; Yu, J. W. *Macromolecules* **1988**, *21*, 484–493.
(54) Forster, S.; Schmidt, M.; Antonietti, M. *Polymer* **1990**, *31*, 781–792.
(55) Mattoussi, H.; Karasz, F. E.; Langley, K. H. *J. Chem. Phys.* **1990**, *93*, 3593–3603.
(56) Sedlak, M. *J. Chem. Phys.* **1994**, *101*, 10140–10144.
(57) Tong, Y. Y.; Dong, Y. Q.; Du, F. S.; Li, Z. C. *Macromolecules* **2008**, *41*, 7339–7346.
(58) Liu, X. M.; Wang, L. S.; Wang, L.; Huang, J. C.; He, C. B. *Biomaterials* **2004**, *25*, 5659–5666.
(59) Orofino, T. A.; Flory, P. J. *J. Phys. Chem.* **1959**, *63*, 283–290.
(60) Chu, B.; Ying, Q.; Lee, D. C.; Wu, D. Q. *Macromolecules* **1985**, *18*, 1962–1972.
(61) Huglin, M. B. *Light Scattering From Polymer Solutions*; Academic Press: New York, 1972.
(62) Zhang, J. W.; Buffle, J. *J. Colloid Interface Sci.* **1995**, *174*, 500–509.
(63) Reith, D.; Muller, B.; Muller-Plathe, F.; Wiegand, S. *J. Chem. Phys.* **2002**, *116*, 9100–9106.
(64) Ying, Q. C.; Wu, G. W.; Chu, B.; Farinato, R.; Jackson, L. *Macromolecules* **1996**, *29*, 4646–4654.
(65) Chu, B. *Laser Light Scattering: Basic Principles and Practice*, 2nd ed.; Academic Press: New York, 1991.
(66) Sedlak, M. *J. Chem. Phys.* **1996**, *105*, 10123–10133.
(67) Zhou, Z. K.; Chu, B.; Peiffer, D. G. *Macromolecules* **1993**, *26*, 1876–1883.
(68) Price, C.; Chan, E. K. M.; Mobbs, R. H.; Stubbersfield, R. B. *Eur. Polym. J.* **1985**, *21*, 355–360.
(69) Baranovsky, V. Y.; Litmanovich, A. A.; Papisov, I. M.; Kabanov, V. A. *Eur. Polym. J.* **1981**, *17*, 969–979.
(70) Osada, Y. *J. Polym. Sci., Polym. Chem.* **1979**, *17*, 3485–3498.